AGU PUBLICATIONS

Global Biogeochemical Cycles

RESEARCH ARTICLE
10.1002/2014GB004935

Key Points:
- Novel in situ measurements of marine particle-associated microbial respiration
- Particle sinking velocities and microbial respiration rates vary by region
- These processes affect the regional efficiency of the ocean's biological pump

Correspondence to:
A. M. P. McDonnell,
amcdonnell@alaska.edu

Citation:
McDonnell, A. M. P., P. W. Boyd, and K. O. Buesseler (2015), Effects of sinking velocities and microbial respiration rates on the attenuation of particulate carbon fluxes through the mesopelagic zone, *Global Biogeochem. Cycles*, *29*, 175–193, doi:10.1002/2014GB004935.

Received 11 JUL 2014
Accepted 2 JAN 2015
Accepted article online 8 JAN 2015
Published online 25 FEB 2015

Effects of sinking velocities and microbial respiration rates on the attenuation of particulate carbon fluxes through the mesopelagic zone

A. M. P. McDonnell[1], P. W. Boyd[2,3], and K. O. Buesseler[4]

[1]School of Fisheries and Ocean Sciences, University of Alaska Fairbanks, Fairbanks, Alaska, USA, [2]Institute for Marine and Antarctic Studies, University of Tasmania, Hobart, Tasmania, Australia, [3]NIWA Centre for Chemical and Physical Oceanography, Department of Chemistry, University of Otago, Dunedin, New Zealand, [4]Department of Marine Chemistry and Geochemistry, Woods Hole Oceanographic Institution, Woods Hole, Massachusetts, USA

Abstract The attenuation of sinking particle fluxes through the mesopelagic zone is an important process that controls the sequestration of carbon and the distribution of other elements throughout the oceans. Case studies at two contrasting sites, the oligotrophic regime of the Bermuda Atlantic Time-series Study (BATS) and the mesotrophic waters of the west Antarctic Peninsula (WAP) sector of the Southern Ocean, revealed large differences in the rates of particle-attached microbial respiration and the average sinking velocities of marine particles, two parameters that affect the transfer efficiency of particulate matter from the base of the euphotic zone into the deep ocean. Rapid average sinking velocities of 270 ± 150 m d^{-1} were observed along the WAP, whereas the average velocity was 49 ± 25 m d^{-1} at the BATS site. Respiration rates of particle-attached microbes were measured using novel RESPIRE (REspiration of Sinking Particles In the subsuRface ocEan) sediment traps that first intercepts sinking particles then incubates them in situ. RESPIRE experiments yielded flux-normalized respiration rates of 0.4 ± 0.1 day^{-1} at BATS when excluding an outlier of 1.52 day^{-1}, while these rates were undetectable along the WAP (0.01 ± 0.02 day^{-1}). At BATS, flux-normalized respiration rates decreased exponentially with respect to depth below the euphotic zone with a 75% reduction between the 150 and 500 m depths. These findings provide quantitative and mechanistic insights into the processes that control the transfer efficiency of particle flux through the mesopelagic and its variability throughout the global oceans.

1. Introduction

Particles sinking from the euphotic zone transport carbon and other elements into the ocean's interior at a global rate of 4–13 Pg C yr^{-1} [*Lima et al.*, 2014] as part of a process known as the "biological pump" [*Volk and Hoffert*, 1985]. This downward flux of particulate organic matter (POM) typically declines sharply with increasing depth due to the activity of particle-attached microbes, physical processes of aggregation and disaggregation, and the consumption or fragmentation of POM by zooplankton [*Simon et al.*, 2002; *Steinberg et al.*, 2008; *Wilson et al.*, 2008; *Burd and Jackson*, 2009]. Variation in the attenuation of particle flux with respect to depth, and the depths at which carbon is remineralized in the water column, can have a substantial impact on the global air-sea balance of carbon dioxide [*Kwon et al.*, 2009] and the global oceanic distributions of many other associated elements. Direct measurements of particle fluxes and inverse modeling studies of tracer distributions indicate that particle flux attenuation and the associated remineralization processes vary significantly with respect to region and season [*Berelson*, 2001; *Francois et al.*, 2002; *Lutz et al.*, 2002; *Howard et al.*, 2006; *Buesseler and Boyd*, 2009]; however, the physical and ecological controls on flux attenuation are poorly understood and difficult to quantify [*Wassmann et al.*, 2003; *Boyd and Trull*, 2007; *Dehairs et al.*, 2008; *Stukel et al.*, 2014]. This situation confounds our ability to accurately describe the role of the biological pump in global biogeochemical cycles and how these processes might respond to and modulate global climate and biogeochemical change.

Conceptually, the balance between particle sinking velocities and the rates of particle remineralization and retention in mesopelagic waters sets the attenuation of particle flux with depth. Both sinking velocities and particle remineralization rates are highly variable and are influenced by a variety of environmental variables and ecosystem properties [*Stemmann et al.*, 2004; *Trull et al.*, 2008; *Iversen and Ploug*, 2010; *McDonnell and Buesseler*, 2010]. Factors such as ambient temperature, particle composition and structure, and community

structure are thought to play a significant role in controlling sinking velocities and rates of particle destruction, thereby influencing the efficiency of the biological carbon pump [*De La Rocha and Passow*, 2007].

Compared to bulk seawater, marine particles (especially marine snow aggregates) are hot spots of microbial activity in the oceans [*Alldredge and Gotschalk*, 1990; *Simon et al*., 1990; *Azam and Long*, 2001]. Remineralization rates of particulate carbon by particle-attached microbes are difficult to quantify and have long been an issue of considerable debate. Discrepancies between different studies likely arise from a combination of substantial variability in these rates throughout the oceans combined with significant methodological differences between studies. Some early studies concluded that marine snow is a relatively poor site for the active remineralization of organic matter, and therefore, microbial degradation of sinking aggregates should be a minor factor in the attenuation of particle fluxes with depth [*Ducklow et al*., 1982; *Alldredge and Youngbluth*, 1985; *Karl et al*., 1988]. Other studies found quite the opposite, however, calculating that POM could be broken down on short timescales of hours to days [*Smith et al*., 1992; *Ploug et al*., 1999; *Ploug and Grossart*, 2000]. Recent experimental results with laboratory-generated aggregates from various phytoplankton cultures have indicated that carbon-specific respiration rates for marine particles average around 0.13 day^{-1}, while the variability around this mean approached a similar magnitude [*Iversen and Ploug*, 2010]. Uncertainties in the magnitude of microbial respiration rates make it very difficult to reconcile carbon budgets in the subsurface ocean [*Burd et al*., 2010; *Giering et al*., 2014] and predict how microbial respiration might be affected by ongoing climate change [*Passow and Carlson*, 2012].

A wide range of techniques has been used for estimating the effects of microbial respiration associated with sinking particles. Many studies have employed thymidine incorporation measurements to assess bacterial production rates [*Chin-Leo and Kirchman*, 1988]. For this reason, relating these measurements to the remineralization of particulate matter is difficult because it requires the use of several poorly constrained conversion factors such as the relative abundances of free-living versus particle-attached microbes, as well as bacterial growth efficiencies [*Rivkin and Legendre*, 2001; *Burd et al*., 2010]. Alternatively, by probing the diffusive boundary layer surrounding aggregates with microelectrodes [*Ploug and Jørgensen*, 1999], laboratory studies have provided valuable insights into the magnitude of microbial remineralization of particulate carbon and the factors that control it [*Ploug et al*., 2008; *Iversen and Ploug*, 2010, 2013]. However, measurements of particle sinking velocities and particle-associated microbial respiration rates have only rarely been combined with oceanographic assessments of flux attenuation [e.g., *Iversen et al*., 2010], limiting our ability to assess their role in setting the efficiencies of the ocean's biological pump.

In this study, we investigate the combined roles of particle-associated microbial respiration and the average sinking velocities of particles in the water column in the control of particle flux attenuation through the mesopelagic zone. This was accomplished with an in situ particle incubation chamber (P. W. Boyd et al., RESPIRE: An in situ particle interceptor to conduct particle remineralization and microbial dynamics studies in the oceans' twilight zone, submitted to *Limnology and Oceanography: Methods*, 2014) and determinations of the relationship between particle flux and concentration [*McDonnell and Buesseler*, 2010]. These experimentally determined rates are compared to the attenuation of particle flux as measured by surface-tethered sediment traps deployed at multiple depths below the euphotic zone. Observations conducted in the Sargasso Sea at the Bermuda Atlantic Time-series Study (BATS) site and along the west Antarctic Peninsula (WAP) provide two distinctly different examples of the global variability in sinking velocities and microbial activity, and the effects these processes have on the efficiency of the biological carbon pump.

2. Materials and Methods

2.1. Study Sites

Studies of sinking velocities, microbial respiration of sinking particles, and flux attenuation were conducted in two contrasting oceanic environments of BATS and WAP (Table 1). Five process studies at the BATS site (31° 40′N, 64°10′W) in the Sargasso Sea are presented here. This region of the subtropical North Atlantic Ocean has been part of intensive oceanographic studies over the past several decades through several long-term scientific programs including BATS [*Michaels and Knap*, 1996; *Steinberg et al*., 2001], the Oceanic Flux Program [*Conte et al*., 2001], Hydrostation S [*Michaels and Knap*, 1996], and the Bermuda Testbed Mooring [*Dickey et al*., 2001]. This site is characterized by seasonally low productivity and deep mixing in the winter followed by a brief spring bloom as the hydrography transitions to a thermally stratified and

Table 1. General Characteristics of the Two Contrasting Study Sites of BATS and WAP

	BATS	WAP
Dominant phytoplankton	Prochlorophytes, cyanobacteria, prymnesiophytes, pelagophytes, coccolithophores, and diatoms	Diatoms, cryptophytes, and flagellates
Dominant zooplankton	Copepods, ostracods, and chaetognaths	Krill, salps, copepods, and pteropods
Dominant sinking particle types	Detrital aggregates and larvacean houses, planktonic sarcodines, and fecal pellets	Krill and salp fecal pellets, diatoms, and aggregates
Seasonality	Peak NPP in winter/early spring and occasional fall bloom	Production and export flux occurring almost entirely in summer
NPP	154 ± 29 gC m^{-2} yr^{-1}[a]	176 gC m^{-2} yr^{-1} (occurring almost exclusively between November and April)[b]
Export ratio	0.06 ± 0.02[a]	0.1[c]

[a] *Lomas et al.* [2013].
[b] *Ducklow et al.* [2008].
[c] *Buesseler et al.* [2010].

nutrient-poor euphotic zone that lasts well into October [*Steinberg et al.*, 2001]. During the summer months, primary production rates decrease and a subsurface chlorophyll maximum develops near the base of the euphotic zone. A diverse assemblage of phytoplankton inhabits the euphotic zone here, dominated by prokaryotic picoplankton such as prochlorophytes and cyanobacteria, but with variable contributions from eukaryotic plankton such as prymnesiophytes, pelagophytes, and coccolithophores [*Steinberg et al.*, 2001]. Sinking particle fluxes in the mesopelagic zone have been measured regularly with surface-tethered free-drifting sediment trap arrays with export ratios (primary production:particulate organic carbon flux at 150 m depth) with a mean *e*-ratio of 0.06 ± 0.02 [*Lomas et al.*, 2013]. The ratio of particulate organic carbon (POC) flux at 300 m to the POC flux at 150 m depths (a measure of the efficiency of flux transfer through the mesopelagic zone) is variable ranging between 0.2 and 0.8, with a statistically significant negative trend between 1996 and 2007 that has been attributed to climate-related shifts in phytoplankton community composition [*Lomas et al.*, 2010].

A set of three experiments was conducted at two locations along the WAP: the Long-Term Ecological Research (LTER) trap site (64°29.3′S, 65°57.6′W, 8–10 January and 5–7 March 2009) 130 km offshore in the midshelf region and at the head of Marguerite Bay (MB) farther to the south (68°10.5′S, 69°59.8′W, 23–25 February 2009). The WAP is a seasonally productive ecosystem with large blooms of diatoms, cryptophytes, and flagellates that constitute the majority of total phytoplankton cell abundance and biomass concentration during the austral summer [*Garibotti et al.*, 2005]. This intense productivity supports large stocks of krill, salps, silverfish, penguins, and marine mammals [*Fraser and Trivelpiece*, 1996; *Ducklow et al.*, 2007]. It is the site of the Palmer Long-Term Ecological Research study (PAL) and other studies that provide an oceanographic context to the measurements presented here. Particle fluxes along the WAP are highly seasonal, often varying over an order of magnitude between the dark and ice-covered winters and highly productive summers [*Ducklow et al.*, 2008; *Weston et al.*, 2013]. These studies also estimated extremely low export ratios (~1%, <4%) with particle flux data derived from seabed-tethered conical time series sediment traps, suggesting that bacteria and zooplankton efficiently recycle particulate matter in the upper water column as it sinks to depth. However, a study with drifting sediment traps and water column profiles of ^{234}Th suggests that particle fluxes are approximately twentyfold larger than those measured by the moored conical trap in this region, resulting in revised export ratios of at least 10% [*Buesseler et al.*, 2010]. Collections of particles in polyacrylamide gel traps revealed that krill fecal pellets and diatom aggregates dominate the flux during the summer months in this region [*McDonnell and Buesseler*, 2010].

2.2. Downward Particle Flux Measurements

To quantify the downward particle flux as a function of depth, surface-tethered free-drifting sediment trap arrays were deployed at each study site. Duplicate cylindrical sediment trap tubes, each with a cross-sectional area, A_{trap}, of 0.0114 m^2 (see Table 2 for a comprehensive list of parameters used in this study), were deployed at three fixed depths below the surface euphotic zone [*Lamborg et al.*, 2008; *McDonnell and Buesseler*, 2012]. Trap depths (Table 3) were selected adaptively at each site such that they were located below the euphotic zone as determined by the decline in conductivity-temperature-depth (CTD)-measured

Table 2. List of Parameters, Their Description, and Units

Parameter	Description	Units
A_{trap}	Cross-sectional area of sediment trap	m^2
c_n	Concentration size distribution	No. m^{-3} μm^{-1}
d	Particle size	μm
F_C	Particulate carbon flux	mmol C m^{-2} d^{-1}
F_C^0	Particulate carbon flux at the base of the euphotic zone	mmol C m^{-2} d^{-1}
F_n	Flux size distribution	No. m^{-2} d^{-1} μm^{-1}
F_{vol}	Volume flux distribution	μm^3 m^2 d^{-1}
n_c	Particulate carbon collected in sediment trap	mmol C
Q_{10}	Temperature coefficient	–
$r_{control}$	Oxygen consumption rate of the particle-excluding RESPIRE trap control	mmol O_2 d^{-1}
r_{exp}	Oxygen consumption rate of the particle-collecting RESPIRE trap experiment	mmol O_2 d^{-1}
r_m	Difference between r_{exp} and $r_{control}$	mmol O_2 d^{-1}
r_{zoop}	Oxygen consumption rate of zooplankton	mmol O_2 d^{-1}
R_m	Flux-normalized particle microbial remineralization rate	day^{-1}
R_m^0	Flux-normalized particle microbial remineralization rate at the base of the euphotic zone	day^{-1}
t_{coll}	Flux collection duration	day
T_{100}	Flux transfer efficiency	–
w	Average sinking velocity size distribution	m d^{-1}
$\overline{w}$	Bulk average sinking velocity	m d^{-1}
λ	Exponential rate of flux attenuation	m^{-1}
$\nu_{C:O_2}$	Stoichiometric ratio of organic carbon to oxygen	–

fluorescence obtained with the CTD. The exact depth placement of the upper traps was limited to 25 m depth intervals at WAP and 50 m intervals at BATS due to the fixed line segments available for the drifting array. The traps were outfitted with lids that were programmed to close after a ~36 h collection phase. Formalin-poisoned brine (500 mL, salinity 70, 0.02% formalin) was added to the base of these flux collection tubes to prevent microbial breakdown of the samples. After the traps were recovered, the particulate matter was allowed to settle for 1 h before the seawater overlying the brine was siphoned off in the shipboard laboratory. The brine and particle sample mixture was then drained through a 350 μm Nitex screen to remove swimmers. Studies at the BATS site showed that there was no difference in removal of swimmers using this screening method versus individual removal of swimmers under a microscope [*Owens et al.*, 2013]. The screened brine suspension was filtered through a 1.2 μm silver membrane filter (Sterlitech), and the particles dried for ~24 h at 50°C. The filtered samples from each trap were analyzed on a CHN analyzer to determine the quantity of carbon collected in the sediment trap, n_c (mmol C), and the reported values are the average of the two duplicate trap tubes. Particulate carbon flux, F_C (mmol C m^{-2} d^{-1}), was calculated by dividing this value by the duration of the collection period and the cross-sectional collection area of the cylindrical traps. At WAP, the 350 μm screen retained many of the large krill fecal pellets collected in the traps. For this reason, zooplankton were handpicked from the screens, and the screened particles (mainly cylindrical fecal pellets) were rinsed off onto a separate silver membrane filter for CHN analysis. Values of n_c and F_C at WAP therefore represent the sum of the $<$350 μm and $>$350 μm size fractions (after removal of swimmers).

2.3. Determination of Average Sinking Velocities

The average sinking velocity of particles as a function of equivalent spherical diameter between 73 μm and ~6 mm was calculated by combining measurements of the particle flux size distribution, F_n, and the particle concentration size distribution, c_n, as described in detail in *McDonnell and Buesseler* [2010, 2012]. Polyacrylamide gel traps were used to collect intact sinking particles for microscopy and the subsequent determination of F_n (No. m^{-2} d^{-1} μm^{-1}). Gel trap tubes were deployed on the same drifting arrays as the flux collection tubes. Methodological details of the polyacrylamide gel traps are covered in McDonnell and Buesseler [*McDonnell and Buesseler*, 2010, 2012]. The autonomous video plankton recorder was used to quantitatively image particles in the water column and compute c_n (No. m^{-3} μm^{-1}) in the depth bin

AGU Global Biogeochemical Cycles

10.1002/2014GB004935

Table 3. Results From RESPIRE Experiments Conducted at BATS and WAP Sites

Site	Date	Depth (m)	Average C Flux (mmol C m^{-2} d^{-1})	Collected During (day)	r_{exp} (mmol O_2 d^{-1})	$r_{control}$ (mmol O_2 d^{-1})	r_{zoop}[a] (mmol O_2 d^{-1})	r_m (mmol O_2 d^{-1})	R_m (day^{-1})
BATS	19–21 April 2008[c]	150	0.85	1.29	0.28 ± 0.02	0.014 ± 0.015	0.003 ± 0.001	0.26 ± 0.03	1.7 ± 0.4
		300	0.54		0.11 ± 0.01	0.014 ± 0.015	0.003 ± 0.001	0.09 ± 0.02	0.9 ± 0.3
		500	0.76		0.068 ± 0.008	0.014 ± 0.015	0.003 ± 0.001	0.051 ± 0.02	0.4 ± 0.2
BATS	12–14 November 2008	150	0.95	1.66	0.011 ± 0.004	-0.001 ± 0.002	0.003 ± 0.001	0.010 ± 0.005	0.4 ± 0.2
BATS	14–16 July 2009	200	4.09	1.52	0.076 ± 0.002	0.030 ± 0.001	0.003 ± 0.001	0.043 ± 0.002	0.4 ± 0.1
		300	2.5						
		500	1.84						
BATS	10–12 September 2009	200	3.88	1.43	0.049 ± 0.002	0.012 ± 0.003	0.003 ± 0.001	0.034 ± 0.004	0.4 ± 0.1
		200	3.88	1.43	0.066 ± 0.002	0.012 ± 0.003	0.003 ± 0.001	0.051 ± 0.004	0.6 ± 0.1
		300	2.78						
		500	1.80						
BATS	21–23 September 2009	200	2.07	1.48	0.054 ± 0.004	0.029 ± 0.001	0.003 ± 0.001	0.021 ± 0.005	0.4 ± 0.1
		200	2.07	1.48	0.047 ± 0.003	0.029 ± 0.001	0.003 ± 0.001	0.015 ± 0.003	0.3 ± 0.1
		300	1.58						
		500	1.21						
BATS	25–27 September 2009	200	2.64	1.51	0.102 ± 0.003	0.000 ± 0.002	0.003 ± 0.001	0.100 ± 0.004	1.5 ± 0.4
		500	1.85						
WAP-LTER	8–10 January 2009	50	12.45	1.45	0.007 ± 0.001	0.004 ± 0.002	0	0.003 ± 0.002[b]	0.01 ± 0.01[b]
		150	8.2						
		250	12.6						
WAP-MB	23–25 February 2009	100	1.7	1.36	−0.001 ± 0.000	−0.004 ± 0.000	0	0.002 ± 0.001[b]	0.08 ± 0.02[b]
		200	1.75						
		300	6.15						
WAP-LTER	5–7 March 2009	50	8.6	1.50	−0.013 ± 0.002	−0.010 ± 0.001	0	−0.003 ± 0.002[b]	−0.01 ± 0.01[b]
		150	8.0						
		250	7.15						

[a]See section 2.2 for details on the estimation of r_{zoop} at BATS. No estimates of r_{zoop} were available from WAP and assumed to be zero due to the fact that most zooplankton along WAP were too large to enter the incubation chamber around the IRS.

[b]Values of r_m are below the detection limit of 0.008 mmol O_2 d^{-1}.

[c]In the April 2008 RESPIRE experiments, RESPIRE traps and their associated flux collection traps were deployed with collection funnels used to amplify the collection of particulate carbon and increase the ability to detect r_{exp} in the incubation chamber at deeper depths. Because all three available RESPIRE instruments were being utilized for flux collection experiments at this time, the control rate, $r_{control}$, assumed to be the average of all other control rates measured at the BATS site.

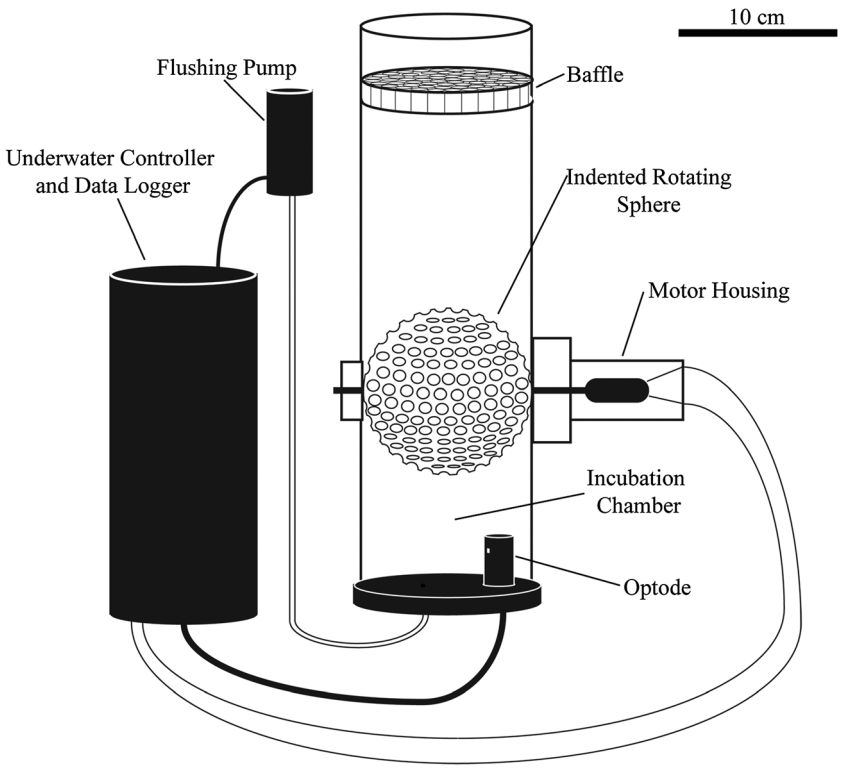

Figure 1. Schematic drawing of the RESPIRE apparatus used to incubate sinking particles and measure the rates of particle-associated microbial respiration.

immediately above each polyacrylamide gel trap. For each size class, d, the flux size distribution was divided by the concentration size distribution giving an average sinking velocity size distribution, $w(d)$, in m d^{-1}:

$$w(d) = F_n(d)/c_n(d) \tag{1}$$

We then computed an estimate of the volume flux, $F_{\text{vol}}(d)$, by summing up the volumes of individual particles in each size class. To accomplish this, we assumed that each particle detected in the polyacrylamide gel images was spherical and thus its volume can be calculated as

$$V_{\text{particle}} = \frac{\pi}{6} d^3 \tag{2}$$

This volumetric flux distribution was then used to weight each $w(d)$ and compute a bulk average sinking velocity, $\overline{w}$, for all particles in the measurable size range as follows:

$$\overline{w} = \frac{\sum (w(d) \cdot F_{\text{vol}}(d))}{\sum F_{\text{vol}}(d)} \tag{3}$$

We compute and report an average $\overline{w}$ across all three depths sampled by the polyacrylamide gels traps in the upper mesopelagic zone.

2.4. In Situ Incubation of Sinking Particles

The respiration rates of particle-attached microbes were measured with an in situ incubation device called the RESPIRE particle interceptor (Figure 1). This instrument and its various uses and methodological concerns are described in further detail in P. W. Boyd et al. (submitted manuscript, 2014). The RESPIRE interceptor used in this study consisted of a modified sediment trap tube made of transparent acrylic and outfitted with a baffle across the top aperture and an indented rotating sphere (IRS) [*Peterson et al.*, 1993] made out of solid PVC plastic that served as both a swimmer avoidance device and the physical closure between the incubation chamber below the IRS and the ambient water above (Figure 1). An Optode (Aanderaa Data Instruments, model 3830) mounted inside the incubation chamber of the RESPIRE traps enabled the measurement of a

dissolved oxygen concentration time series during the deployment. Control of the instrument and Optode was handled by a dedicated computer and battery pack contained in a pressure-tight underwater housing. Up to three RESPIRE traps were deployed simultaneously on the drifting sediment trap array and mounted on the trap frames adjacent to the flux collection tubes and the polyacrylamide gel traps. In all but one of the deployments (April 2008), all RESPIRE traps were deployed at the depth of the upper trap, just below the base of the euphotic zone. Two of the RESPIRE traps served as particle-incubating replicates, while one of the RESPIRE traps was covered with a 10 μm nylon mesh to exclude sinking particles to provide an in situ procedural control. In the 19–21 April 2008 deployment (Table 3), the RESPIRE traps were deployed at three different depths below the euphotic zone in order to determine the change in particle-attached respiration rates through the water column. Larger collection funnels ($A_{trap} = 0.0965\ m^2$) were fitted to the top of the RESPIRE and flux collection tubes during the 19–21 April 2008 deployment to amplify the collection of particles from these deployments and enable the detection of respiration rates in the deeper traps where the flux is diminished.

In all deployments, the RESPIRE traps operated in two modes: the collection phase (corresponding with the collection phase of the adjacent flux collection and polyacrylamide tubes) and the incubation phase. Prior to deployment of the sediment trap arrays, the RESPIRE traps were filled with 0.2 μm filtered seawater collected using the CTD rosette from the depth of the planned deployment. In the case of the September 2009 deployments at BATS, an underwater CTD pump flushed the incubation chambers of the RESPIRE traps with an excess (~5 L) of ambient seawater immediately after deployment at depth (Figure 1). The purpose of this flushing was to increase the stability of the initial oxygen concentrations at the start of the collection phase with those of ambient waters.

During the collection phase, sinking particles entered the opening of the trap and settled onto an IRS machine out of solid PVC [*Peterson et al*., 1993]. An external controller rotated the IRS for 50 s (approximately one complete rotation) every 10 min, thereby transferring any particles collected on top of the IRS into a 1.34 L incubation chamber below. Particles then settled onto the flat PVC base plate of the RESPIRE trap's incubation chamber. During this collection period, IRS rotation also promoted the exchange of ambient seawater into the incubation chamber.

After a collection period, t_{coll}, of ~36 h, the incubation phase began with the closure of the trap lid and the cessation of the IRS rotation. This prevented additional particles from entering the chamber and also further isolated the incubation chamber from fluid exchange with ambient waters. The factory-calibrated Optode measured the concentration of dissolved oxygen in the incubation chamber once every 2 min. Unlike typical oxygen electrodes, they rely on dynamic luminescence quenching by molecular oxygen and therefore do not consume the analyte. After the closure of the trap lids at the conclusion of the collection phase, oxygen concentrations were monitored in the incubation chamber for a period of 4 h prior to instrument recovery.

Linear regressions were performed on these data to determine the rates of decline in the oxygen concentration, and this rate was multiplied by the volume of the incubation chamber (1.34 L) to yield oxygen consumption rates (mmol O_2 day^{-1}) for the particle-collecting experiment (r_{exp}) and particle-excluding control ($r_{control}$). Although the IRS design of the RESPIRE trap was intended to exclude mesozooplankton from the incubation chamber, small zooplankton were occasionally able to enter the incubation chamber during the periodic IRS rotations, and their respiration (r_{zoop}) is also responsible for a portion of the observed drawdown in oxygen. From these rates, we determined a flux-normalized particle microbial remineralization rate, R_m (day^{-1}) calculated with the following equation:

$$R_m = \frac{\left(r_{exp} - r_{control} - r_{zoop}\right) v_{C:O_2}}{F_c t_{coll} A_{trap}} \quad (4)$$

where $v_{C:O_2} = 117/170$ is the stoichiometric ratio of organic carbon to oxygen for organic matter remineralized at depth [*Anderson and Sarmiento*, 1994]. R_m is therefore the fraction of the total accumulated carbon that is remineralized by particle-associated microbes over the course of 1 day. Several studies have confirmed that carbon-specific remineralization rates are largely independent of aggregate size [*Iversen et al*., 2010; *Ploug et al*., 1999; *Ploug and Grossart*, 2000], providing justification for the normalization of oxygen consumption rates to the total flux of carbon entering the trap.

Table 4. Flux-Normalized Particle Microbial Remineralization Rates, R_m^0, Calculated From Equation (1) and Bulk Average Sinking Velocities, $\overline{w}$, Determined at the Two Test Sites[a]

Location	Date	R_m^0 (day^{-1})	$\overline{w}$ (m d^{-1})	T_{100}^{model}	T_{100}^{traps}
BATS	12–14 November 2008	0.4 ± 0.2	–	–	–
	14–16 July 2009	0.4 ± 0.1	13 ± 4	0.07	0.61
	10–12 September 2009	0.5 ± 0.2	90 ± 50	0.65	0.71
	21–23 September 2009	0.4 ± 0.1	23 ± 5	0.28	0.87
	25–27 September 2009	1.5 ± 0.4	70 ± 20	0.18	–
WAP	8–10 January 2009	0.01 ± 0.01	91 ± 43	0.99	0.68
	23–25 February 2009	0.04 ± 0.02	112 ± 55	0.97	1.02
	5–7 March 2009	−0.01 ± 0.01	640 ± 440	1.00	0.93

[a]The modeled flux attenuation only accounts for the combined effects of microbial respiration and sinking.

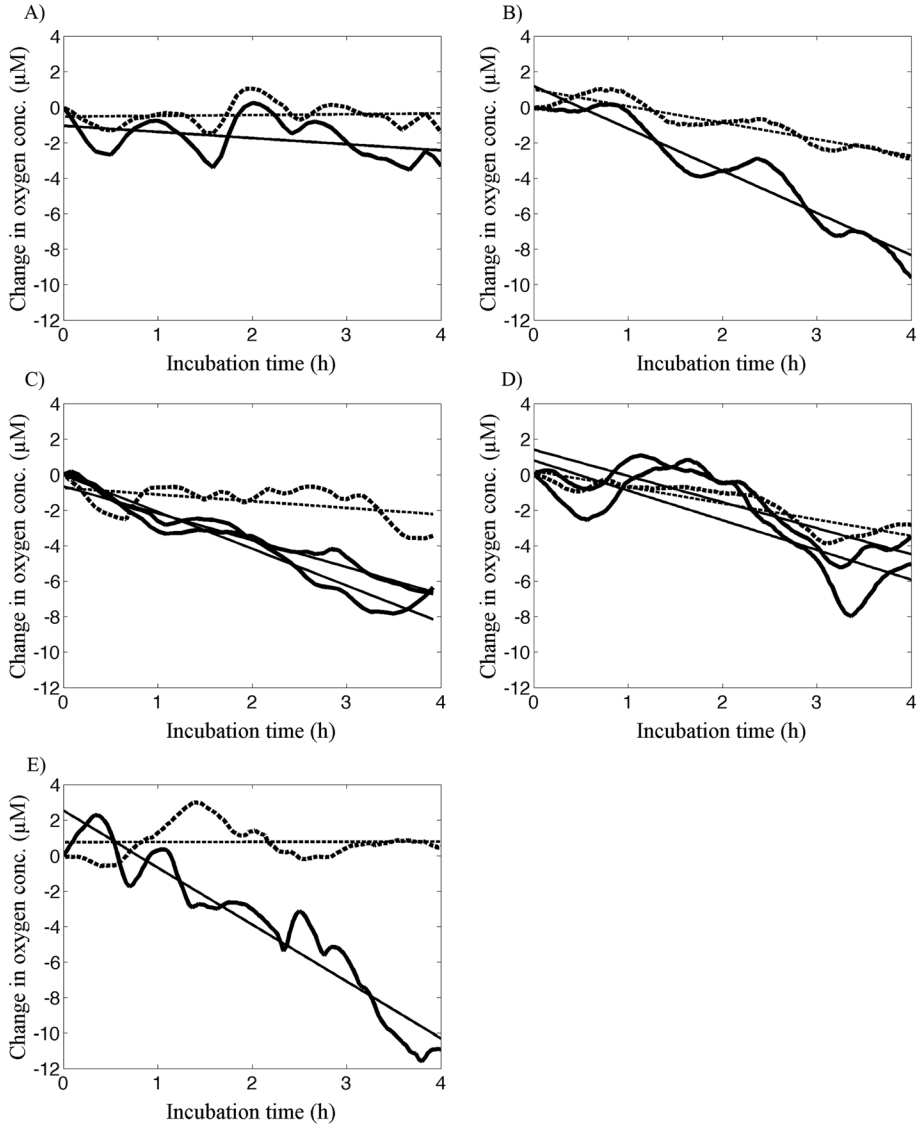

Figure 2. The changes in oxygen concentrations during the incubation phases of the (a) 12–14 November 2008, (b)14–16 July 2009, (c) 10–12 September 2009, (d) 21–23 September 2009, and (e) 25–27 September 2009 RESPIRE experiments conducted at the BATS site. The dashed curves indicate the oxygen changes in the 10 μm mesh-covered (particle-excluding) control. The solid curves are the oxygen changes in the particle-collecting RESPIRE traps. Plotted in the same shading are the linear fits of r_{exp} and $r_{control}$ for each respective experiment. Figures 2c and 2d contain results from side-by-side replicates of the particle-collecting RESPIRE experiments.

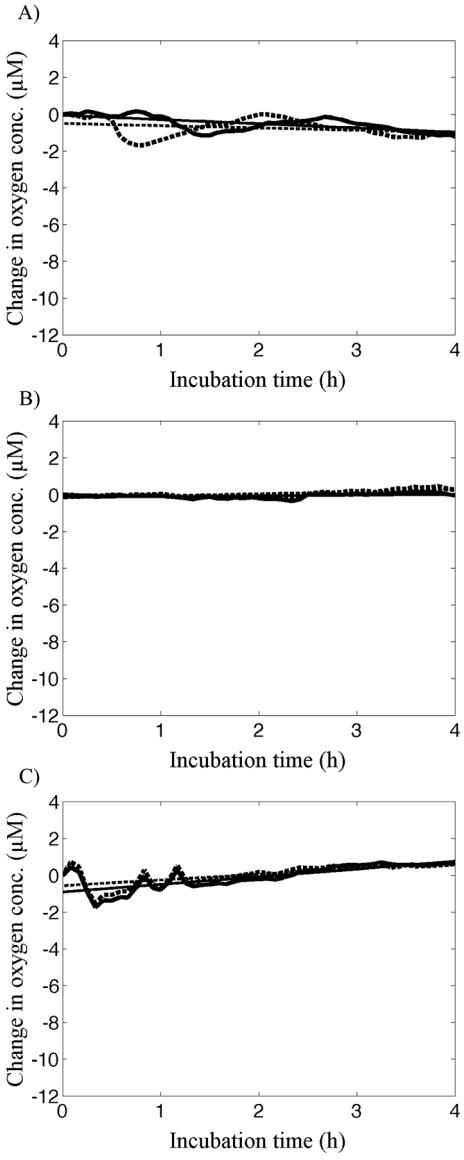

Figure 3. The changes in oxygen concentrations during the incubation phases of the (a) 8–10 January 2009, (b) 23–25 February 2009, and (c) 5–7 March 2009 RESPIRE experiments conducted along the WAP. The dashed curves indicate the oxygen changes in the 10 μm mesh-covered (particle-excluding) control. The solid curves are the oxygen changes in the particle-collecting RESPIRE traps. Plotted in the same shading are the linear fits of r_{exp} and $r_{control}$ for each respective experiment. Figures 3a and 3c took place at the PAL trap site, while Figure 3b was conducted at the mouth of Marguerite Bay (see section 2.5).

While zooplankton data were not available from the specific RESPIRE trap experiments reported here, we did enumerate zooplankton swimmers collected during a series of RESPIRE test deployments in the summer of 2008 at BATS and used these counts to calculate an average zooplankton oxygen consumption rate for RESPIRE collections at BATS. Applying the formulation of zooplankton metabolic rates reported in *Ikeda et al.* [2001] and the average individual dry weights of the subtropical copepod Corycaeus sp. (0.032 mg dry weight/individual), we calculated an average zooplankton oxygen consumption rate for RESPIRE collections at BATS of $r_{zoop} = 0.003 \pm 0.001$ mmol O_2 d^{-1}. At WAP, we assumed r_{zoop} to be negligible, as the majority of the dominant zooplankton species (salps, pteropods, and krill) was too large to pass by the IRS. The errors for R_m were calculated by propagating the uncertainties from r_{exp}, $r_{control}$, and r_{zoop} and n_c. In future RESPIRE deployments, we recommend that zooplankton within the traps be enumerated every time as standard procedure so that r_{zoop} can be determined uniquely for each experiment and thereby avoiding the errors associated with using a fixed estimate of this term.

2.5. Assessment of Mesopelagic Transfer Efficiency

We adopted the metric of transfer efficiency, T_{100} [*Buesseler and Boyd*, 2009], where

$$T_{100} = (\text{flux 100 m below Ez})/(\text{flux at Ez}) \quad (5)$$

and Ez denotes the depth of the euphotic zone. As defined, T_{100} is a measure of flux attention just below Ez and does not suffer from using fixed depths to parameterize flux attenuation, which fails when Ez is variable in time or between sites.

3. Results

3.1. Flux-Weighted Average Sinking Velocities

At BATS, $\overline{w}$ ranged from 13 to 90 m d^{-1} (Table 4) and averaged 49 ± 25 m d^{-1}. Particles sank much more quickly along the WAP, with $\overline{w}$ ranging from 91 to 620 m d^{-1} (Table 4) with an average of 270 ± 150 m d^{-1}. The variability in $\overline{w}$ between deployments at the BATS site appears to be primarily driven by changes in the water column particle concentration. In July 2009, when the average sinking velocity was at its lowest (13 m d^{-1}), the particle concentrations in all size classes were the highest observed at this site, while the flux size distribution was very similar to that observed in other deployments. Along the WAP, the difference in average sinking velocities at the LTER trap site was due to differences in both the particle concentration and flux. The high-sinking velocities of particles observed in the WAP are likely attributable to the fact that the flux is dominated by fast-sinking diatom aggregates and krill fecal pellets [*McDonnell and Buesseler*, 2010]. In contrast, the particles collected in the polyacrylamide gel traps at BATS were mostly small, semitransparent aggregates. In addition, water column particle concentrations throughout the mesopelagic zones were

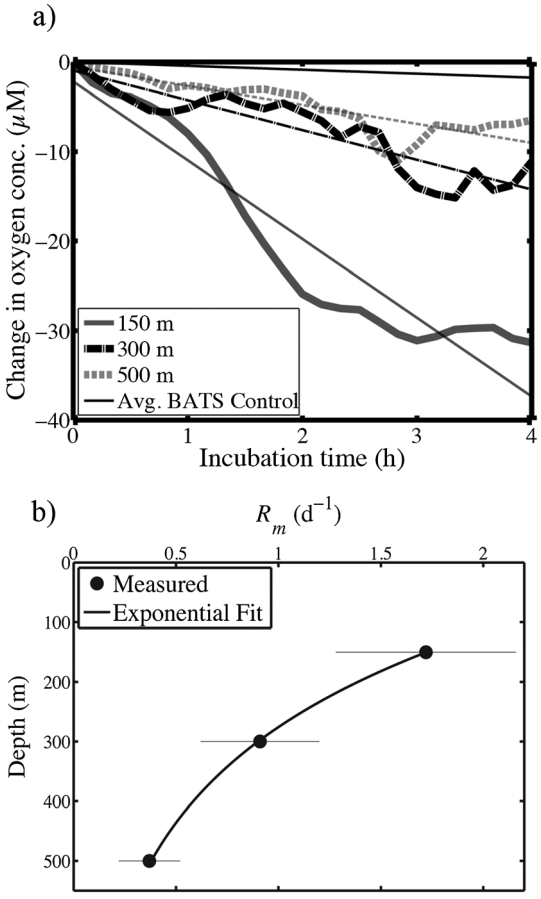

Figure 4. (a) Oxygen drawdown in the RESPIRE traps deployed at three depths throughout the mesopelagic zone at the BATS station in April 2008. The lines represent the linear fit to each respective experiment as well as the average rate of oxygen consumption in all of the BATS particle-excluding controls. (b) The flux-normalized microbial respiration rates (R_m) as a function of depth at BATS with an exponential fit to the data (equation (6)).

actually higher at BATS than they were at WAP despite generally lower fluxes at the former. This implies that many of the particles in the water column at BATS were either sinking very slowly or not at all.

3.2. Flux-Normalized Respiration Rates

Five controlled experiments were conducted at the BATS site and three along the WAP (Table 3). The plots in Figures 2 and 3 show the changes in oxygen concentration that occurred in the incubation chambers during the 4 h incubation phase that followed ~ 36 h of particle interception. The divergence between the particle-excluding control (dotted lines) and the particle-collecting incubators (solid lines) can be attributed to the microbial respiration associated with the sinking particles, as the particle-excluding mesh cover is the only difference between the two configurations. The BATS deployments had a divergence of 1–10 μM over the course of the 4 h incubation (Figure 2). Incubations along the WAP showed no significant divergence from the particle-excluding control (Figure 3). Replicate particle-collecting RESPIRE experiments were conducted at BATS during the 10–12 and 21–23 September 2009, providing measures of the uncertainty in any individual RESPIRE experiment. These replicates yielded an average standard deviation in the slope of the oxygen time series of 0.3 μM O_2 h^{-1} (equivalent to 0.006 mmol O_2 d^{-1}). For r_m, this equates to an average standard deviation of 0.008 mmol O_2 d^{-1} between replicates, a value that we define as the lower detection limit of the RESPIRE experiments.

Flux-normalized measurements of microbial remineralization rates at the base of the euphotic zone, R_m^0, were calculated from this oxygen data (Table 3). At BATS, R_m^0 ranged from 0.3 to 1.5 day^{-1} with an average value of 0.57 day^{-1} (for the experiments conducted with procedural controls). Data from the 25–27 September 2009 RESPIRE deployment at BATS appear to be an outlier, with an R_m^0 of approximately threefold larger than those from the other six controlled experiments at this site. Excluding this outlier gives an average R_m^0 of 0.4 ± 0.1 day^{-1} at BATS. In the case of the three WAP deployments, r_m, the differences between the oxygen drawdown in the particle-collecting and particle-excluding controls were below the RESPIRE detection limit of 0.008 mmol O_2 d^{-1} (Table 3). For this reason, R_m^0 was deemed undetectable for all three deployments along the WAP, with an average rate of 0.01 ± 0.02 day^{-1}. R_m^0 was statistically different between the two sites (BATS and WAP) with $p < 0.05$.

Inspection of the polyacrylamide gels deployed along the WAP revealed no visual change in the quality or structural integrity of material caught at different depths. Specifically, intact diatom cells and aggregates were observed and krill fecal pellets remained tightly encased in their peritrophic membranes at all depths [*McDonnell and Buesseler*, 2010], supporting the conclusion that microbial activity had a negligible effect on these particles during their rapid transit to depth at WAP.

In situ particle-associated respiration rates were also measured at multiple depths at BATS (Table 3). Figure 4a shows the results from an experiment with three RESPIRE traps each deployed at 150, 300, and 500 m

depths at the BATS site in April 2008. On an absolute basis, the decline in dissolved oxygen concentration in the incubation chamber decreased most rapidly in the shallow trap, and progressively decreasing respiration rates were detected in traps deployed at greater depths. In this deployment configuration, all three RESPIRE traps were located at different depths, and therefore, there were no RESPIRE instruments available to operate as controls. In this case, the average oxygen decline in the mesh-covered controls at the BATS site was used (Figure 4a, gray line). We found that flux-normalized respiration rates decreased rapidly through the mesopelagic zone, with a 78% reduction in R_m from 1.72 day^{-1} at 150 m to 0.37 day^{-1} at 500 m (Figure 4b and Table 3). This decline in R_m was fit with an exponential decay function

$$R_m(z) = R_m^0 e^{-\lambda z} \tag{6}$$

yielding a λ of 0.0043 m^{-1}.

3.3. Flux Attenuation

The differences in particle sinking velocities and microbial respiration rates have significant implications for the sequestration of carbon in the subsurface ocean. At BATS, the measurements of low-sinking velocities and high remineralization rates would be expected to produce strong attenuation of flux through the water column. By contrast, with no detectable particle-associated microbial respiration of particulate matter and relatively fast sinking velocities, attenuation of WAP fluxes due to these processes would be negligible.

Using $\overline{w}$, R_m^0 at the upper trap depth, and depth-dependent scaling of $R_m(z)$ from the April 2008 BATS deployment, and the average measured flux at the upper trap depth, we modeled the attenuation of flux with respect to depth for each deployment at BATS and WAP. The purpose of this simplistic model is to assess the role of variability in sinking velocities and microbial respiration on flux attenuation. By comparing this model to the flux profiles obtained from the drifting sediment trap arrays, we aim to evaluate the relative importance of these two rates in the control of flux attenuation. Many other processes such as zooplankton activity and physical aggregation and fragmentation of particles will also play a role in the overall flux attenuation [*Stukel et al*., 2014] and thus are likely responsible for the residuals between the modeled and observed fluxes. The modeled sinking and microbial respiration flux profiles $F(z)$ were computed as follows:

$$F_C(z) = F_C^0 e^{-(z-z_0)R_m(z)/\overline{w}} \tag{7}$$

where F_C^0 is the flux measured at the upper trap depth (z_0) [*Volk and Hoffert*, 1985]. Starting with the measured trap flux and R_m^0 at the upper trap depth, the flux was computed iteratively down through the water column using equation (7). Note that in each case we applied the measured R_m^0 from that particular site and sediment trap deployment, but this value was scaled as a function of depth according to equation (6) and the λ value we measured at BATS during the April 2008 deployments at multiple depths. Given the very low R_m^0 at WAP, the model at this site is insensitive to the choice of λ.

This modeled flux attenuation curves, $F_C(z)$, were compared to the flux profiles obtained from the drifting sediment trap arrays. Given the fact that $\overline{w}$ is computed as the ratio between the flux and the concentration of all particles in the water column (which includes both sinking and suspended particles), $\overline{w}$ is a lower limit estimate of the velocity of the actively sinking particles as the presence of suspended particles would decrease $\overline{w}$. For this reason, $F_C(z)$ is expected to be an upper limit estimate of flux attenuation.

Figures 5a–5d show the measured sediment trap fluxes at BATS plotted along with the flux attenuation profiles as computed with the model. In the four deployments at BATS, the sinking and remineralization model predicted similar or stronger flux attenuation than what was measured by sediment traps. The 10–12 September study predicted the 300 and 500 m fluxes within 10% of those measured by the sediment traps. Particle flux measurements and modeled fluxes for the WAP are reported in Figures 5e–5g. Sediment trap measurements (Table 3) in this region showed no clear patterns of decreasing flux with respect to depth, and in some cases, carbon fluxes even increased at depths below about 200 m, possibly due to zooplankton activity and the vertical shunt or lateral inputs of particles [*Palanques et al*., 2002]. The lack of observed flux attenuation is consistent with the observed measurements of particle-attached microbial activity and average sinking velocities. The modeled fluxes are unchanged with respect to depth because the microbial respiration rates determined with the RESPIRE traps were undetectable.

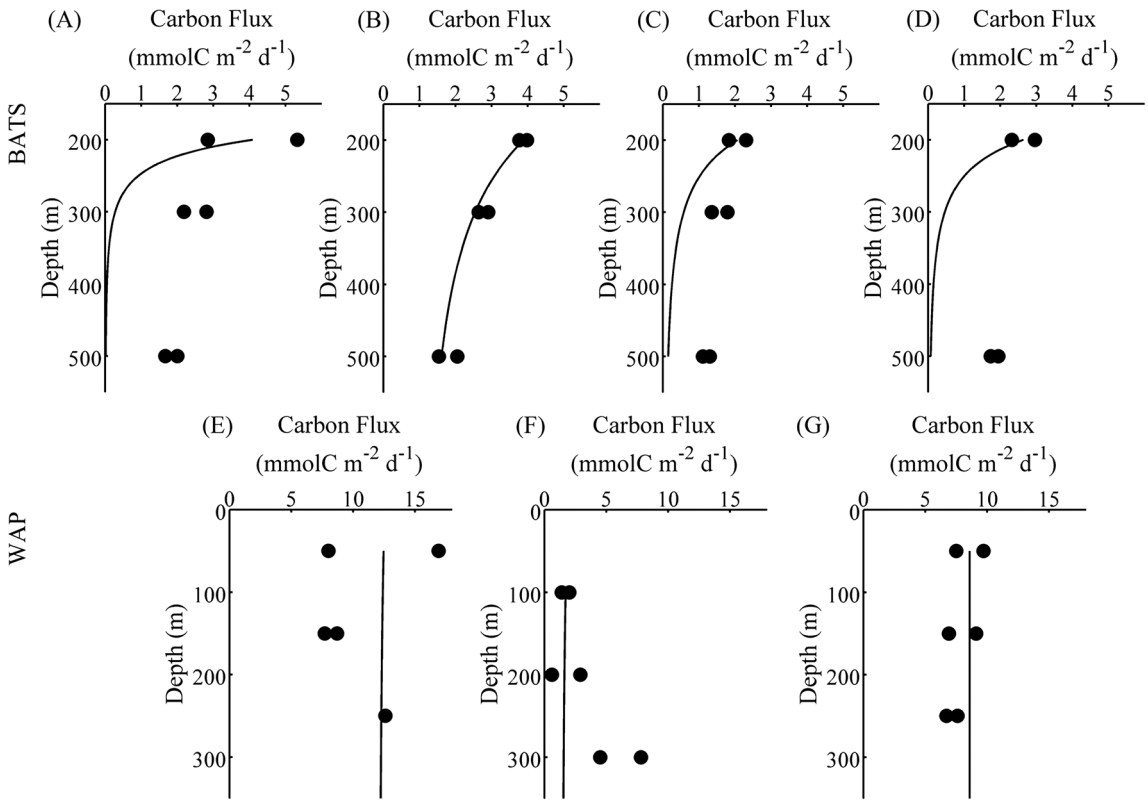

Figure 5. Particulate carbon fluxes plotted as a function of depth for both the (a–d) BATS sites and (e–g) along the WAP. Panels include deployments on 14–16 July 2009 (Figure 5a), 10–12 September 2009 (Figure 5b), 21–23 September 2009 (Figure 5c), 25–27 September 2009 (Figure 5d), 8–10 January 2009 (Figure 5e), 23–25 February 2009 (Figure 5f), and 5–7 March 2009 (Figure 5g). The points represent the measurements made with individual trap tubes on the surface-drifting sediment traps. The curves plot the flux attenuation profiles modeled from measurements of the bulk average sinking velocities and the flux-normalized microbial respiration rates.

We compared the modeled and measured transfer efficiencies T_{100} (Table 4) and calculated an R^2 value of only 0.29 and a p value of 0.21.

In order to determine the relative contributions of R_m^0 and $\overline{w}$ to changes in flux attenuation, we conducted a simple sensitivity experiment with equation (7). Starting with $R_m^0 = 0.4\ \text{day}^{-1}$ and $\overline{w} = 100\ \text{m d}^{-1}$, we calculated that a 1% change in R_m^0 and $\overline{w}$ resulted in a −0.32% and 0.32% change in T_{100}, respectively. Thus, variability in both R_m^0 and $\overline{w}$ affect T_{100} in equal but opposite manners. Our observations from BATS and WAP indicate that there were larger relative variations in R_m^0 between the two sites, and as a result, variability in this parameter had the largest effect on the differences in T_{100}. In fact, with essentially no respiration occurring on the particles at WAP, $\overline{w}$ did not influence the modeled flux attenuation at that site. Given the unknown global variability in R_m^0 and $\overline{w}$, additional measurements of both rates are necessary to determine if the relative variability in R_m^0 is always the dominant factor as we observed at these two sites.

3.4. Global Context

The relationships between NPP, flux at the base of the euphotic zone, and flux 100 m below the euphotic zone for several sites throughout the oceans are illustrated in Figure 6. The Ez ratio represents the fraction of NPP exported out of the base of the euphotic. This figure, modified from *Buesseler and Boyd* [2009], includes the average fluxes for BATS and WAP presented in this study. Estimates of NPP were obtained from the BATS and PAL online databases. WAP has one of the highest average T_{100} values at 0.87, corresponding to very little attenuation of flux beneath the euphotic zone, and only a modest average Ez ratio of 0.17. In contrast, BATS exhibited a T_{100} of 0.66 and an Ez ratio of 0.09. The labeled contours in Figure 6 denote the percentage of NPP that reaches 100 m below the base of the euphotic zone, with about 15% at WAP and just over 5% at BATS.

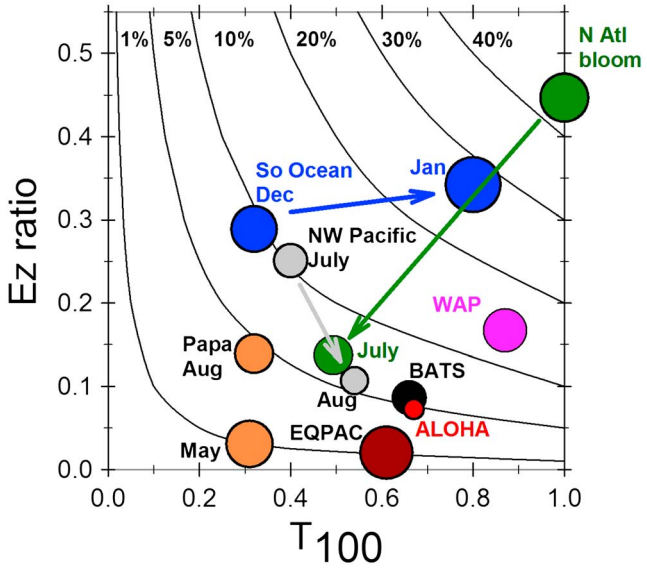

Figure 6. Comparison of export and flux attenuation properties at various study sites throughout the global oceans, adapted from *Buesseler and Boyd* [2009]. Data from this study are included from BATS and WAP. The contour lines represent the percentage of NPP that reaches depths 100 m below the base of the euphotic zone. The area of each circle is proportional to the NPP at that site.

4. Discussion

The two study sites of BATS and WAP offer strongly contrasting examples of how particle-associated microbial activity and particle sinking velocities can vary throughout the oceans and how these rates affect the regional efficiency of the biological carbon pump of the oceans. Figure 6 demonstrates that the WAP site is overall much more efficient at sequestering carbon due to its larger T_{100} and Ez ratios. WAP lies near one global end-member in terms of T_{100} with almost no observed flux attenuation in the mesopelagic, similar to the North Atlantic spring bloom and January observations from another Southern Ocean site. In this property space, BATS has very similar biological pump properties as station ALOHA in the oligotrophic North Pacific Ocean and suggests that other oligotrophic sites may present similar biological pump characteristics. Similar to BATS and ALOHA, ~5% of NPP reaches depths 100 m below the base of the euphotic at other midlatitude sites during the summer such as station PAPA in August, the North Atlantic in July, and the NW Pacific in August, although these efficiencies are accomplished with a combination of slightly lower T_{100} and higher Ez ratios.

The observed differences in microbial respiration rates are likely due to several different factors. Cold, polar waters such as those along the WAP are recognized as regions of low bacterial production rates likely due to a combination of low temperatures, low availability of labile organic matter, and low bacterial biomass [*Pomeroy and Deibel*, 1986; *Wiebe et al*., 1992; *Kirchman et al*., 2009] relative to low-latitude sites such as BATS. Subsurface water temperatures along the WAP are characteristic of the Upper Circumpolar Deep Water that intrudes onto the continental shelf at temperatures only a few degrees above freezing [*Ducklow et al*., 2007], which could contribute to slower respiration rates at WAP. Bacterial biomass and production may also be limited at WAP due to top-down control through bacterial grazing and viral lysis. In support of this hypothesis, *Bird and Karl* [1999] found high abundances of bacteriovores along the WAP that led to suppressed bacterial abundance and metabolism.

In addition to the ecological attributes of the microbial community at WAP, other factors related to the nature of the particulate substrates may be important in slowing the activity of particle-associated microbes at these sites. *Hansen et al*. [1996] found that fecal pellets formed from a diet of diatoms (like those at the WAP sites) were more recalcitrant to microbial degradation than those formed from nanoflagellate or dinoflagellate diets (common at BATS) due to the more robust mechanical structure of the fecal matter derived from diatom diets. A pronounced peritrophic membrane that encases the partially digested diatomaceous material also enhances the resistance of the krill fecal pellets to microbial colonization and decomposition [*Turner and Ferrante*, 1979], rendering these pellets efficient vehicles for the transfer of organic matter into deeper waters. Furthermore, the opal matrix associated with the diatomaceous particulate matter could serve to protect the labile organic carbon from microbial breakdown [*Mayer*, 1994; *Armstrong et al*., 2001], thereby retarding microbial respiration along the WAP. These properties of recalcitrant particulate matter are supported by our own observations that the fecal pellets and diatom aggregates collected in the polyacrylamide gel traps at WAP were in visually similar structural condition at all depths sampled, confirming that there was little physical degradation of this material on its transit through the water column.

Interestingly, the observation that R_m^0 is higher at BATS than at WAP differs from the generalizations of several previous studies that high-latitude regions with large seasonality of particle production and export are sites of more highly labile planktonic particles and relatively strong remineralization and flux attenuation [*Arístegui et al*., 1996, 2005; *Francois et al*., 2002; *Henson et al*., 2012]. A recent investigation using neutrally buoyant sediment traps found instead that mesopelagic flux attenuation was greatest in low-latitude warm waters [*Marsay et al*., 2015], a finding that is consistent with the flux observations and rate measurements reported here.

With bathymetry along the WAP shelf averaging 430 m, and an average sinking velocity of 270 m d^{-1}, sinking particles will take an average of ~1.6 day to reach the seafloor, thereby offering little time for particle-attached microbes to remineralize a significant proportion of the particulate matter during its transit to the seafloor. Indeed, large quantities of particulate organic matter in the form of fecal pellets and phytodetritus are deposited on the WAP shelf sediments during summer peak flux events, and this flux supports a rich benthos throughout the year [*Mincks et al*., 2005; *Smith et al*., 2008].

As discussed above, the errors reported in Table 3 are calculated using the average uncertainty in both the magnitude of the trap flux and the average uncertainty in the slope of the oxygen concentration as a function of time. The availability of only three RESPIRE instruments for a given deployment and occasional RESPIRE operational issues resulted in limited opportunities to replicate particle-collecting experiments and particle-excluding controls. However, the few duplicates that we did obtain (Table 3) indicated only a small amount of variability in the oxygen consumption rates during a given experiment on a single trap array, providing confidence that the observed variability between successive deployments was indeed real, and the general pattern of higher R_m^0 rates at BATS relative to the WAP was reproducible and statistically significant. Our observations that WAP particles are subjected to very little microbial degradation during their descent through the water column are supported by other observations in this region. Leucine incorporation experiments with unpoisoned sediment trap samples in the Bransfield Strait region indicated microbial degradation rates of less than 1% per day [*Anadón et al*., 2002] and were found to be consistent with low rates of water column respiration [*Varela et al*., 2002]. Similarly, *Weston et al*. [2013] found minimal remineralization of particulate fluxes at depths greater than 200 m in Marguerite Bay.

Although we were only able to make a single deployment with RESPIRE traps operated at multiple depths, the observed reduction in R_m as a function of depth (Figure 4) is an important finding and one that should be investigated more thoroughly in future studies. Many biogeochemical models of ocean flux to depth rely on the assumption that particle remineralization rates do not change as particles move deeper through the water column [*Gieskes*, 1983; *Gruber et al*., 2006; *Buesseler and Boyd*, 2009], while others employ sinking velocities that increase with respect to depth in order to better fit the observed flux attenuation profiles [*Schmittner et al*., 2005; *Kriest and Oschlies*, 2008]. If R_m does decrease with respect to depth, as observed here, this could also explain why the shape of the particle flux attenuation profiles are well characterized by an empirical power law fit [*Martin et al*., 1987; *Boyd and Trull*, 2007]. An accurate understanding of the shape of flux to depth is important because this parameter determines the distribution of carbon and nutrients throughout the oceans and the air-sea balance of carbon dioxide [*Lutz et al*., 2002; *Howard et al*., 2006; *Kwon et al*., 2009]. Furthermore, partitioning the flux attenuation mechanism correctly between the drivers of R_m and $\overline{w}$ is necessary to assess how flux attenuation and oceanic carbon sequestration is affected by other dynamic processes such as the lateral transport and global climate change.

The mechanism for the decline in R_m with respect to depth was not assessed in this study; however, this depth-dependent decrease is greater than would be expected solely from the effect of colder water temperatures at the deeper trap depths. The observed decline in R_m at BATS from 1.72 day^{-1} at 150 m to 0.37 day^{-1} at 500 m would imply a Q_{10} temperature coefficient of over 2×10^3 given the observed temperature difference of 2°C between those depths; however, this temperature sensitivity is unrealistically 3 orders of magnitude too high when compared to those of laboratory experiments involving marine snow aggregates which suggest a Q_{10} of ~3.5 [*Iversen and Ploug*, 2013]. Thus, processes other than temperature control of respiration rates must play a role in the retardation of R_m with respect to depth. Increasing pressures experienced by attached microbial communities have been shown to slow rates of leucine and thymidine incorporation [*Turley*, 1993], an effect that would have been captured by our in situ RESPIRE experiments at various depths. Another possibility is that as particulate carbon is remineralized on its transit to depth, only the more refractory components are left behind and the microbial rates decline at depth as abundance

of labile material is reduced [*Turley and Stutt*, 2000; *Lutz et al*., 2002]. Enzymatic hydrolysis of particulate organic matter has been shown to decrease rapidly in the zone immediately below the euphotic zone, and given the tight coupling between hydrolysis and utilization of organic matter by microbes [*Hoppe et al*., 1993; *Huston and Deming*, 2002], declining hydrolysis rates with respect to depth may be a rate-limiting step for microbial respiration of sinking particulate matter.

As discussed in section 3.4, the fact that $F_C(z)$ overestimates the degree of attenuation measured by the sediment traps is expected since our use of $\overline{w}$ is a description of the average sinking velocity of all particles in the water column which includes both sinking and suspended particles. This is because the presence of any suspended particulate matter in the water column would lead to an underestimate of the sinking velocities of the actively sinking pool and therefore an overestimation of flux attenuation. In addition to this expected bias, the use of a single $\overline{w}$ to describe the sinking behavior of a collection of particles has its limitations because marine particles sink across a wide spectrum of velocities [*Armstrong et al*., 2009; *Alonso-Gonzalez et al*., 2010]. If the spectrum of sinking velocities is not well characterized by its average, this variability could induce uncertainties in the model of flux to depth. Furthermore, by averaging the measured sinking velocities across the three depths at which they were measured, it may mask some of the vertical variability in the average sinking velocities. However, we observed no distinct trends or patterns in the vertical distribution of sinking velocities that would have a large impact on the modeled flux profiles.

In addition, there are several other possible explanations why flux profiles modeled with only sinking velocities and microbial respiration rates predicted more rapid flux attenuation than measured by the sediment trap arrays. Diel vertical migration of zooplankton can create a vertical shunt of particulate matter from the euphotic zone or other upper layers into the mesopelagic zone [*Boyd et al*., 1999; *Steinberg et al*., 2000]. This would bypass the typical settling and decomposition pathway described in this simple microbial length scale model and lead to fluxes in the deep traps that would be larger than expected from the high measured rates of microbial activity, as we observed at BATS. The vertical shunt could also account for the sporadic increases in particle flux that were observed at depths $>$ 200 m along the WAP (Figure 5), especially given the presence of krill swarms [*Lascara et al*., 1999].

Microbes associated with marine snow also communicate with each other through signaling molecules using quorum sensing [*Gram and Grossart*, 2002; *Hmelo and Van Mooy*, 2009]. Given the enclosed nature of the incubation chambers, it is also possible that the concentrations of labile substrates and quorum sensing signaling molecules could accumulate to levels that induce quorum sensing behavior and lead to artificially high measured rates of microbial activity. Furthermore, in this experimental design, there is a temporal disconnect of 0–36 h between the collection of particles in the chamber and the measurement of the associated microbial respiration rates (P. W. Boyd et al., submitted manuscript, 2014). If microbial activity changes with respect to time, the measured rates could be different from those actually occurring on the particles at the depth it is measured. *Turley and Stutt* [2000] found that cell-specific microbial activity did vary over the first several days after particle collection, so this artifact may play a role in biasing the rate measurements (P. W. Boyd et al., submitted manuscript, 2014).

Several previous studies have found that shallow traps are prone to under collection of sinking fluxes [*Buesseler*, 1991; *Buesseler et al*., 2000]. If the upper trap has a stronger collection bias than the deeper traps due to enhanced lateral currents at the upper depths, this type of bias would reduce the initial (shallow) flux of the model and lead to the underestimation of the modeled deep fluxes, as was observed. Furthermore, it would also lead to low estimates of $F_n(d)$ and therefore $w(d)$ (see equation (2)) which would also accelerate the modeled flux attenuation.

Several other methodological issues were considered, although it is unlikely that these factors had a significant effect on our experimental results because they would cause an underestimation of the modeled flux attenuation with respect to the observed sediment trap flux profiles, a phenomenon that we did not observe. First, because the RESPIRE traps only measure the respiration of particle-attached microbes, the model we applied does not take into account the effects of zooplankton destruction of particles through swimming or the consumption of particles at depth [*Wilson et al*., 2008; *Buesseler and Boyd*, 2009; *Giering et al*., 2014]. These processes are thought to be significant in many places throughout the oceans [*Steinberg et al*., 2008], and their effect would be to enhance flux attenuation relative to sinking and remineralization model applied here. Second, the lack of ambient fluid motion that the particles

experience inside the RESPIRE trap could possibly lead to an underestimation of the carbon-specific remineralization rates (P. W. Boyd et al., submitted manuscript, 2014). In these RESPIRE experiments, the particles settle onto the base plate of the incubation chamber and therefore are no longer in a state of perpetual sinking through the water column. The flow of seawater around sinking particles creates a microenvironment with an accelerated mass transfer between an aggregate and its surroundings [*Kiørboe et al*., 2001; *Ploug*, 2001]. Therefore, the reduction in mass transfer of oxygen toward the particle in the RESPIRE traps may cause an underestimation of respiration rates if particle-attached microbes become oxygen limited while sitting on a surface and without the ambient fluid flow induced by sinking [*Ploug and Jørgensen*, 1999]. However, diffusion limitation of biological processes occurs only when the biological demand for oxygen at the surface of the aggregate exceeds the flux through the diffusive boundary layer. *Iversen et al*. [2010] found that even in stagnant conditions, the O_2 concentration within the aggregates that they tested was >90 μM, and therefore, respiration was not diffusion limited.

5. Conclusions

These results illustrate how the respiration of particle-associated microbes and particle sinking velocities vary significantly between the subtropical Sargasso Sea and the polar/subpolar waters above the WAP continental shelf. Respiration rates of particle-attached microbial communities were substantially higher at BATS than the undetectable rates at WAP. The effect of temperature on microbial respiration rates likely plays a role but was not sufficient to explain the full magnitude of the differences between sites. This suggests that other regional characteristics of the biological carbon pump such as the recalcitrant nature of the zooplankton fecal pellets and diatom aggregates along the WAP may be important in inhibiting the effect of particle-attached microbial degradation on the sinking flux of particulate organic carbon. Moreover, the bulk average sinking velocities at WAP were about 5 times faster than those measured in the Sargasso Sea. Along the WAP, average sinking velocities were fast enough to transport particles from the surface waters down to the seafloor on the continental shelf in a matter of only a couple of days, whereas the majority of particles in the Sargasso Sea would take over 1 week to reach the 500 m depth horizon, giving particle-attached microbes more of an opportunity to remineralize the sinking particulate matter. Thus, regional variability in sinking velocities and microbial respiration rates led to clear regional distinctions in the transfer efficiency of particle flux through the mesopelagic zone, with both observed and modeled flux attenuation almost nonexistent at the WAP site, while fluxes attenuated much more rapidly at BATS. These observations offer important new insights into the factors that control the variability of the biological pump throughout the global oceans. This work is an essential step toward understanding how particle sinking and microbial respiration modulate the global carbon cycle and how these processes might respond to global change.

Acknowledgments

Estimates of NPP for Figure 6 were obtained from the BATS and PAL online databases. All other original data used to create the figures are included in the data tables of this manuscript or can be requested directly from the corresponding author A. McDonnell at amcdonnell@alaska.edu. We thank Palmer LTER and the Food For Benthos on the Antarctic Continental Shelf Project (FOODBANCS) for accommodating our science on their respective cruises to the west Antarctic Peninsula. Funding was provided by the University of Alaska Fairbanks, Woods Hole Oceanographic Institution (WHOI) Rinehart Access to the Sea Program, the WHOI Coastal Oceans Institute, WHOI Academic Programs Office, and the National Science Foundation (NSF) for support of PAL (ANT-0823101), FOODBANCS, and WAPflux (ANT- 83886600) projects. A grant from the NSF Carbon and Water Program (06028416) supported the development of these methods.

References

Alldredge, A. L., and C. C. Gotschalk (1990), The relative contribution of marine snow of different origins to biological processes in coastal waters, *Cont. Shelf Res.*, *10*, 41–58.

Alldredge, A. L., and M. J. Youngbluth (1985), The significance of macroscopic aggregates (marine snow) as sites for heterotrophic bacterial production in the mesopelagic zone of the subtropical Atlantic, *Deep Sea Res., Part I*, *32*(12), 1445–1456.

Alonso-Gonzalez, I. J., J. Aristegui, C. Lee, A. Sanchez-Vidal, A. Calafat, J. Fabres, P. Sangr, P. Masque, A. Hernandez-Guerra, and V. Benitez-Barrios (2010), Role of slowly settling particles in the ocean carbon cycle, *Geophys. Res. Lett.*, *37*, L13608, doi:10.1029/2010GL043827.

Anadón, R., F. Alvarez-Marqués, E. Fernández, M. Varela, M. Zapata, J. Gasol, and D. Vaqué (2002), Vertical biogenic particle flux during austral summer in the Antarctic Peninsula area, *Deep Sea Res., Part II*, *49*, 883–901.

Anderson, L. A., and J. L. Sarmiento (1994), Redfield ratios of remineralization determined by nutrient data analysis, *Global Biogeochem. Cycles*, *8*(1), 65–80, doi:10.1029/93GB03318.

Arístegui, J., M. Montero, and S. Baallesteros (1996), Planktonic primary production and microbial respiration measured by 14C assimilation and dissolved oxygen changes in coastal waters of the Antarctic Peninsula during austral summer: Implications for carbon flux studies, *Mar. Ecol. Prog. Ser.*, *132*(1992), 191–201.

Arístegui, J., S. Agustì, J. J. Middelburg, and C. M. Duarte (2005), Respiration in the mesopelagic and bathypelagic zones of the ocean, *Respir. Aquat. Ecosyst.*, 181–205.

Armstrong, R. A., C. Lee, J. I. Hedges, S. Honjo, and S. G. Wakeham (2001), A new, mechanistic model for organic carbon fluxes in the ocean based on the quantitative association of POC with ballast minerals, *Deep Sea Res., Part II*, *2*(49), 219–236.

Armstrong, R. A., M. L. Peterson, C. Lee, and S. G. Wakeham (2009), Settling velocity spectra and the ballast ratio hypothesis, *Deep Sea Res., Part II*, *56*(18), 1470–1478.

Azam, F., and R. A. Long (2001), Sea snow microcosms, *Nature*, *414*(6863), 495–498.

Berelson, W. M. (2001), The flux of particulate organic carbon into the ocean interior: A comparison of four U.S. JGOFS regional studies, *Oceanography*, *14*(4), 59–67.

Bird, D., and D. Karl (1999), Uncoupling of bacteria and phytoplankton during the austral spring bloom in Gerlache Strait, Antarctic Peninsula, *Aquat. Microb. Ecol.*, *19*(1981), 13–27.

Boyd, P. W., and T. W. Trull (2007), Understanding the export of biogenic particles in oceanic waters: Is there consensus?, *Prog. Oceanogr.*, *72*, 276–312.

Boyd, P. W., N. D. Sherry, J. A. Berges, J. K. B. Bishop, S. E. Calvert, M. A. Charette, S. J. Giovannoni, R. Goldblatt, P. J. Harrison, and S. B. Moran (1999), Transformations of biogenic particulates from the pelagic to the deep ocean realm, *Deep Sea Res., Part II*, *46*(11–12), 2761–2792.

Buesseler, K. O. (1991), Do upper-ocean sediment traps provide an accurate record of particle flux?, *Nature*, *353*(6343), 420–423.

Buesseler, K. O., and P. W. Boyd (2009), Shedding light on processes that control particle export and flux attenuation in the twilight zone of the open ocean, *Limnol. Oceanogr.*, *54*(4), 1210–1232.

Buesseler, K. O., D. K. Steinberg, A. F. Michaels, R. J. Johnson, J. E. Andrews, J. R. Valdes, and J. F. Price (2000), A comparison of the quantity and composition of material caught in a neutrally buoyant versus surface-tethered sediment trap, *Deep Sea Res., Part II*, *47*(2), 277–294.

Buesseler, K. O., A. M. P. McDonnell, O. M. E. Schofield, D. K. Steinberg, and H. W. Ducklow (2010), High particle export over the continental shelf of the west Antarctic Peninsula, *Geophys. Res. Lett.*, *37*, L22606, doi:10.1029/2010GL045448.

Burd, A. B., and G. A. Jackson (2009), Particle aggregation, *Ann. Rev. Mar. Sci.*, *1*, 65–90.

Burd, A. B., D. A. Hansell, D. K. Steinberg, T. R. Anderson, J. Arlstegui, F. Baltar, S. R. BeauprÈ, K. O. Buesseler, F. DeHairs, and G. A. Jackson (2010), Assessing the apparent imbalance between geochemical and biochemical indicators of meso-and bathypelagic biological activity: What the @$#! is wrong with present calculations of carbon budgets?, *Deep Sea Res., Part II*, *57*(16), 1557–1571.

Chin-Leo, G., and D. L. Kirchman (1988), Estimating bacterial production in marine waters from the simultaneous incorporation of thymidine and leucine, *Appl. Environ. Microbiol.*, *54*(8), 1934–1939.

Conte, M. H., N. Ralph, and E. H. Ross (2001), Seasonal and interannual variability in deep ocean particle fluxes at the Oceanic Flux Program (OFP)/Bermuda Atlantic Time Series (BATS) site in the western Sargasso Sea near Bermuda, *Deep Sea Res., Part II*, *48*(8), 1471–1505.

De La Rocha, C. L., and U. Passow (2007), Factors influencing the sinking of POC and the efficiency of the biological carbon pump, *Deep Sea Res., Part II*.

Dehairs, F., A. de Brauwere, and M. Elskens (2008), Organic carbon in the ocean's twilight zone: Controls on organic carbon export and twilight zone remineralization: Brussels, Belgium, 28–30 May 2008, *Eos Trans. AGU*, *89*(38), 351, doi:10.1029/2008EO380004.

Dickey, T., S. Zedler, X. Yu, S. C. Doney, D. Frye, H. Jannasch, D. Manov, D. Sigurdson, J. D. McNeil, and L. Dobeck (2001), Physical and biogeochemical variability from hours to years at the Bermuda Testbed Mooring site: June 1994–March 1998, *Deep Sea Res., Part II*, *48*(8–9), 2105–2140.

Ducklow, H. W., D. L. Kirchman, and G. T. Rowe (1982), Production and vertical flux of attached bacteria in the Hudson River plume of the New York Bight as studied with floating sediment traps, *Appl. Environ. Microbiol.*, *43*(4), 769–776.

Ducklow, H. W., K. Baker, D. G. Martinson, L. B. Quetin, R. M. Ross, R. C. Smith, S. E. Stammerjohn, M. Vernet, and W. Fraser (2007), Marine pelagic ecosystems: The West Antarctic Peninsula, *Philos. Trans. R. Soc. London, Ser. B*, *362*(1477), 67.

Ducklow, H. W., M. Erickson, J. Kelly, M. Montes-Hugo, C. A. Ribic, R. C. Smith, S. E. Stammerjohn, and D. M. Karl (2008), Particle export from the upper ocean over the continental shelf of the west Antarctic Peninsula: A long-term record, 1992–2007, *Deep Sea Res., Part II*, *55*(18–19), 2118–2131.

Francois, R., S. Honjo, R. Krishfield, and S. Manganini (2002), Factors controlling the flux of organic carbon to the bathypelagic zone of the ocean, *Global Biogeochem. Cycles*, *16*(4), 1087, doi:10.1029/2001GB001722.

Fraser, W. R., and W. Z. Trivelpiece (1996), Factors controlling the distribution of seabirds: Winter-summer heterogeneity in the distribution of AdÈlie penguin populations, in *Foundations for Ecological Research West of the Antarctic Peninsula*, vol. 70, edited by R. M. Ross, E. E. Hofmann, and L. B. Quetin, pp. 257–272, AGU, Washington, D. C., doi:10.1029/AR070p0257.

Garibotti, I. A., M. Vernet, and M. E. Ferrario (2005), Annually recurrent phytoplanktonic assemblages during summer in the seasonal ice zone west of the Antarctic Peninsula (Southern Ocean), *Deep Sea Res., Part I*, *52*(10), 1823–1841, doi:10.1016/j.dsr.2005.05.003.

Giering, S. L. C., et al. (2014), Reconciliation of the carbon budget in the ocean's twilight zone, *Nature*, *507*(7493), 480–483, doi:10.1038/nature13123.

Gieskes, J. M. (1983), The chemistry of interstitial waters of deep-sea sediments: Interpretation of deep-sea drilling data, in *Chemical Oceanography*, vol. 8, edited by J. Riley and R. Chester, pp. 221–269, Elsevier, New York.

Gram, L., and H. Grossart (2002), Possible quorum sensing in marine snow bacteria: Production of acylated homoserine lactones by Roseobacter strains isolated from marine snow, *Appl. Environ. Microbiol.*, *68*(8), 4111–4116, doi:10.1128/AEM.68.8.4111.

Gruber, N., H. Frenzel, S. C. Doney, P. Marchesiello, J. C. McWilliams, J. R. Moisan, J. J. Oram, G. K. Plattner, and K. D. Stolzenbach (2006), Eddy-resolving simulation of plankton ecosystem dynamics in the California Current System, *Deep Sea Res., Part I*, *53*(9), 1483–1516.

Hansen, B., F. L. L. Fotel, N. J. Jensen, and S. D. Madsen (1996), Bacteria associated with a marine planktonic copepod in culture. II. Degradation of fecal pellets produced on a diatom, a nanoflagellate or a dinoflagellate diet, *J. Plankton Res.*, *18*(2), 275–288, doi:10.1093/plankt/18.2.275.

Henson, S. A., R. Sanders, and E. Madsen (2012), Global patterns in efficiency of particulate organic carbon export and transfer to the deep ocean, *Global Biogeochem. Cycles*, *26*, GB1028, doi:10.1029/2011GB004099.

Hmelo, L., and B. A. S. Van Mooy (2009), Kinetic constraints on acylated homoserine lactone-based quorum sensing in marine environments, *Aquat. Microb. Ecol.*, *54*, 127–133.

Hoppe, H., H. Ducklow, and B. Karrasch (1993), Evidence for dependency of bacterial growth on enzymatic hydrolysis of particulate organic matter in the mesopelagic ocean, *Mar. Ecol. Prog. Ser.*, *93*, 277–283.

Howard, M. T., A. M. E. Winguth, C. Klaas, and E. Maier-Reimer (2006), Sensitivity of ocean carbon tracer distributions to particulate organic flux parameterizations, *Global Biogeochem. Cycles*, *20*, GB3011, doi:10.1029/2005GB002499.

Huston, A., and J. Deming (2002), Relationships between microbial extracellular enzymatic activity and suspended and sinking particulate organic matter: Seasonal transformations in the North Water, *Deep Sea Res., Part II*, *49*(22-23), 5211–5225, doi:10.1016/S0967-0645(02)00186-8.

Ikeda, T., Y. Kanno, K. Ozaki, and A. Shinada (2001), Metabolic rates of epipelagic marine copepods as a function of body mass and temperature, *Mar. Biol.*, *139*(3), 587–596.

Iversen, M. H., and H. Ploug (2010), Ballast minerals and the sinking carbon flux in the ocean: Carbon-specific respiration rates and sinking velocity of marine snow aggregates, *Biogeosciences*, *7*(9), 2613–2624, doi:10.5194/bg-7-2613-2010.

Iversen, M. H., and H. Ploug (2013), Temperature effects on carbon-specific respiration rate and sinking velocity of diatom aggregates—Potential implications for deep ocean export processes, *Biogeosciences*, *10*(6), 4073–4085, doi:10.5194/bg-10-4073-2013.

Iversen, M. H., N. Nowald, H. Ploug, G. A. Jackson, and G. Fischer (2010), High resolution profiles of vertical particulate organic matter export off Cape Blanc, Mauritania: Degradation processes and ballasting effects, *Deep Sea Res., Part I*, *57*(6), 771–784.

Karl, D. M., G. A. Knauer, and J. H. Martin (1988), Downward flux of particulate organic matter in the ocean: A particle decomposition paradox, *Nature*, *332*(6163), 438–441.

Kiørboe, T., H. Ploug, and U. H. Thygesen (2001), Fluid motion and solute distribution around sinking aggregates. I. Small-scale fluxes and heterogeneity of nutrients in the pelagic environment, *Mar. Ecol. Prog. Ser.*, *211*, 1–13.
Kirchman, D. L., X. A. G. Morán, and H. Ducklow (2009), Microbial growth in the polar oceans—Role of temperature and potential impact of climate change, *Nat. Rev. Microbiol.*, *7*(6), 451–459, doi:10.1038/nrmicro2115.
Kriest, I., and A. Oschlies (2008), On the treatment of particulate organic matter sinking in large-scale models of marine biogeochemical cycles, *Biogeosciences*, *5*, 55–72.
Kwon, E. Y., F. Primeau, and J. L. Sarmiento (2009), The impact of remineralization depth on the air-sea carbon balance, *Nat. Geosci.*, *2*(9), 630–635.
Lamborg, C. H., K. O. Buesseler, J. Valdes, C. H. Bertrand, R. Bidigare, S. Manganini, S. Pike, D. Steinberg, T. Trull, and S. Wilson (2008), The flux of bio-and lithogenic material associated with sinking particles in the mesopelagic "twilight zone" of the northwest and North Central Pacific Ocean, *Deep Sea Res., Part II*, *55*(14–15), 1540–1563.
Lascara, C. M., E. E. Hofmann, R. M. Ross, and L. B. Quetin (1999), Seasonal variability in the distribution of Antarctic krill, Euphausia superba, west of the Antarctic Peninsula, *Deep Sea Res., Part I*, *46*(6), 951–984, doi:10.1016/S0967-0637(98)00099-5.
Lima, I. D., P. J. Lam, and S. C. Doney (2014), Dynamics of particulate organic carbon flux in a global ocean model, *Biogeosciences*, *11*(4), 1177–1198, doi:10.5194/bg-11-1177-2014.
Lomas, M. W., D. K. Steinberg, T. Dickey, C. A. Carlson, N. B. Nelson, R. H. Condon, and N. R. Bates (2010), Increased ocean carbon export in the Sargasso Sea linked to climate variability is countered by its enhanced mesopelagic attenuation, *Biogeosciences*, *7*(1), 57–70, doi:10.5194/bg-7-57-2010.
Lomas, M. W., N. R. Bates, R. J. Johnson, A. H. Knap, D. K. Steinberg, and C. A. Carlson (2013), Two decades and counting: 24-years of sustained open ocean biogeochemical measurements in the Sargasso Sea, *Deep Sea Res., Part II*, *93*, 16–32, doi:10.1016/j.dsr2.2013.01.008.
Lutz, M., R. Dunbar, and K. Caldeira (2002), Regional variability in the vertical flux of particulate organic carbon in the ocean interior, *Global Biogeochem. Cycles*, *16*(3), 1037, doi:10.1029/2000GB001383.
Marsay, C. M., R. J. Sanders, S. A. Henson, K. Pabortsava, E. P. Achterberg, and R. S. Lampitt (2015), Attenuation of sinking particulate organic carbon flux through the mesopelagic ocean, *Proc. Natl. Acad. Sci.*, doi:10.1073/pnas.1415311112.
Martin, J. H., G. A. Knauer, D. M. Karl, and W. W. Broenkow (1987), VERTEX: Carbon cycling in the northeast Pacific, *Deep Sea Res., Part I*, *34*(2), 267–285.
Mayer, L. M. (1994), Surface area control of organic carbon accumulation in continental shelf sediments, *Geochim. Cosmochim. Acta*, *58*(4), 1271–1284.
McDonnell, A. M. P., and K. O. Buesseler (2010), Variability in the average sinking velocity of marine particles, *Limnol. Oceanogr.*, *55*(5), 2085–2096.
McDonnell, A. M. P., and K. O. Buesseler (2012), A new method for the estimation of sinking particle fluxes from measurements of the particle size distribution, average sinking velocity, and carbon content, *Limnol. Oceanogr. Meth.*, *10*, 329–346, doi:10.4319/lom.2012.10.329.
Michaels, A. F., and A. H. Knap (1996), Overview of the U.S. JGOFS Bermuda Atlantic Time-series Study and the Hydrostation S program, *Deep Sea Res., Part II*, *43*(2–3), 157–198.
Mincks, S. L., C. R. Smith, and D. J. DeMaster (2005), Persistence of labile organic matter and microbial biomass in Antarctic shelf sediments: Evidence of a sediment food bank, *Mar. Ecol. Prog. Ser.*, *300*, 3–19.
Owens, S. A., K. O. Buesseler, C. H. Lamborg, J. Valdes, M. W. Lomas, R. J. Johnson, D. K. Steinberg, and A. D. Siegel (2013), A new time series of particle export from neutrally buoyant sediments traps at the Bermuda Atlantic Time-series Study site, *Deep Sea Res., Part I*, *72*, 34–47, doi:10.1016/j.dsr.2012.10.011.
Palanques, A., E. Isla, P. Puig, J. A. Sanchez-Cabeza, and P. Masqué (2002), Annual evolution of downward particle fluxes in the Western Bransfield Strait (Antarctica) during the FRUELA project, *Deep Sea Res., Part II*, *49*(4–5), 903–920, doi:10.1016/S0967-0645(01)00130-8.
Passow, U., and C. Carlson (2012), The biological pump in a high CO_2 world, *Mar. Ecol. Prog. Ser.*, *470*(2), 249–271, doi:10.3354/meps09985.
Peterson, M. L., P. J. Hernes, D. S. Thoreson, J. I. Hedges, C. Lee, and S. G. Wakeham (1993), Field evaluation of a valved sediment trap, *Limnol. Oceanogr.*, *38*(8), 1741–1761.
Ploug, H. (2001), Small-scale oxygen fluxes and remineralization in sinking aggregates, *Limnol. Oceanogr.*, *46*(7), 1624–1631.
Ploug, H., and B. B. Jørgensen (1999), A net-jet flow system for mass transfer and microsensor studies of sinking aggregates, *Mar. Ecol. Prog. Ser.*, *176*(1), 279.
Ploug, H., and H. P. Grossart (2000), Bacterial growth and grazing on diatom aggregates: Respiratory carbon turnover as a function of aggregate size and sinking velocity, *Limnol. Oceanogr.*, *45*(7), 1467–1475.
Ploug, H., H. P. Grossart, F. Azam, and B. B. Joergensen (1999), Photosynthesis, respiration, and carbon turnover in sinking marine snow from surface waters of Southern California Bight: Implications for the carbon cycle in the ocean, *Mar. Ecol. Prog. Ser.*, *179*, 1–11.
Ploug, H., M. Iversen, and G. Fischer (2008), Ballast, sinking velocity, and apparent diffusivity within marine snow and zooplankton fecal pellets: Implications for substrate turnover by attached bacteria, *Limnol. Oceanogr.*, *53*, doi:10.4319/lo.2008.53.5.1878.
Pomeroy, L. R., and D. Deibel (1986), Temperature regulation of bacterial activity during the spring bloom in Newfoundland coastal waters, *Science*, *233*(4761), 359–361, doi:10.1126/science.233.4761.359.
Rivkin, R. B., and L. Legendre (2001), Biogenic carbon cycling in the upper ocean: Effects of microbial respiration, *Science*, *291*(5512), 2398–2400, doi:10.1126/science.291.5512.2398.
Schmittner, A., A. Oschlies, X. Giraud, M. Eby, and H. L. Simmons (2005), A global model of the marine ecosystem for long-term simulations: Sensitivity to ocean mixing, buoyancy forcing, particle sinking, and dissolved organic matter cycling, *Global Biogeochem. Cycles*, *19*, GB3004, doi:10.1029/2004GB002283.
Simon, M., A. L. Alldredge, and F. Azam (1990), Bacterial carbon dynamics on marine snow, *Mar. Ecol. Prog. Ser.*, *65*, 205–211.
Simon, M., H. P. Grossart, B. Schweitzer, and H. Ploug (2002), Microbial ecology of organic aggregates in aquatic ecosystems, *Aquat. Microb. Ecol.*, *28*(2), 175–211.
Smith, C. R., S. Mincks, and D. J. DeMaster (2008), The FOODBANCS project: Introduction and sinking fluxes of organic carbon, chlorophyll-a and phytodetritus on the western Antarctic Peninsula continental shelf, *Deep Sea Res., Part II*, *55*(22–23), 2404–2414, doi:10.1016/j.dsr2.2008.06.001.
Smith, D. C., M. Simon, A. L. Alldredge, and F. Azam (1992), Intense hydrolytic enzyme activity on marine aggregates and implications for rapid particle dissolution, *Nature*, *359*(6391), 139–142.
Steinberg, D. K., C. A. Carlson, N. R. Bates, S. A. Goldthwait, L. P. Madin, and A. F. Michaels (2000), Zooplankton vertical migration and the active transport of dissolved organic and inorganic carbon in the Sargasso Sea, *Deep Sea Res., Part I*, *47*, 137–158.
Steinberg, D. K., C. A. Carlson, N. R. Bates, R. J. Johnson, A. F. Michaels, and A. H. Knap (2001), Overview of the U.S. JGOFS Bermuda Atlantic Time-series Study (BATS): A decade-scale look at ocean biology and biogeochemistry, *Deep Sea Res., Part II*, *48*(8), 1405–1447.

Steinberg, D. K., B. A. S. Van Mooy, K. O. Buesseler, P. W. Boyd, T. Kobari, and D. M. Karl (2008), Bacterial vs. zooplankton control of sinking particle flux in the ocean's twilight zone, *Limnol. Oceanogr.*, *53*(4), 1327–1338.

Stemmann, L., G. A. Jackson, and D. Ianson (2004), A vertical model of particle size distributions and fluxes in the midwater column that includes biological and physical processes—Part I: Model formulation, *Deep Sea Res., Part I*, *51*, 865–884.

Stukel, M., K. Mislan, M. Décima, and L. Hmelo (2014), Detritus in the pelagic ocean, in *Eco-DAS IX Symposium Proceedings*, edited by P. Kemp, pp. 49–76, Associate for the Sciences of Limnology and Oceanography, Waco, Tex.

Trull, T. W., S. G. Bray, K. O. Buesseler, C. H. Lamborg, S. Manganini, C. Moy, and J. Valdes (2008), In situ measurement of mesopelagic particle sinking rates and the control of carbon transfer to the ocean interior during the Vertical Flux in the Global Ocean (VERTIGO) voyages in the North Pacific, *Deep Sea Res., Part II*, *55*(14–15), 1684–1695.

Turley, C. M. (1993), The effect of pressure on leucine and thymidine incorporation by free-living bacteria and by bacteria attached to sinking oceanic particles, *Deep Sea Res., Part I*, *40*(11), 2193–2206.

Turley, C. M., and E. D. Stutt (2000), Depth-related cell-specific bacterial leucine incorporation rates on particles and its biogeochemical significance in the Northwest Mediterranean, *Limnol. Oceanogr.*, *45*(2), 419–425.

Turner, J. T., and J. G. Ferrante (1979), Zooplankton fecal pellets in aquatic ecosystems, *Bioscience*, *29*(11), 670–677.

Varela, M., E. Fernandez, and P. Serret (2002), Size-fractionated phytoplankton biomass and primary production in the Gerlache and south Bransfield Straits (Antarctic Peninsula) in Austral summer 1995–1996, *Deep Sea Res., Part II*, *49*(4–5), 749–768, doi:10.1016/S0967-0645(01)00122-9.

Volk, T., and M. I. Hoffert (1985), Ocean carbon pumps: Analysis of relative strengths and efficiencies in ocean-driven atmospheric CO_2 changes, in *The Carbon Cycle and Atmospheric CO_2: Natural Variations Archean to Present; Proceedings of the Chapman Conference on Natural Variations in Carbon Dioxide and the Carbon Cycle, Tarpon Springs, Fla., January 9-13, 1984 (A86-39426 18-46)*, Washington, D. C.

Wassmann, P., K. Olli, C. W. Riser, and C. Svensen (2003), Ecosystem function, biodiversity and vertical flux regulation in the twilight zone, in *Marine Science Frontiers for Europe SE-19*, edited by G. Wefer, F. Lamy, and F. Mantoura, pp. 279–287, Springer, Berlin.

Weston, K., T. D. Jickells, D. S. Carson, A. Clarke, M. P. Meredith, M. A. Brandon, M. I. Wallace, S. J. Ussher, and K. R. Hendry (2013), Primary production export flux in Marguerite Bay (Antarctic Peninsula): Linking upper water-column production to sediment trap flux, *Deep Sea Res., Part I*, *75*, 52–66, doi:10.1016/j.dsr.2013.02.001.

Wiebe, W. J., W. M. Sheldon, and L. R. Pomeroy (1992), Bacterial growth in the cold: Evidence for an enhanced substrate requirement, *Appl. Environ. Microbiol.*, *58*(1), 359–364.

Wilson, S. E., D. K. Steinberg, and K. O. Buesseler (2008), Changes in fecal pellet characteristics with depth as indicators of zooplankton repackaging of particles in the mesopelagic zone of the subtropical and subarctic North Pacific Ocean, *Deep Sea Res., Part II*, *55*(14–15), 1636–1647.